Supplementary information for:

Kilowatt average power single-mode laser light transmission over kilometre-scale hollow core fibre

H. C. H. Mulvad[1], S. Abokhamis Mousavi[1], V. Zuba[1], L. Xu[1]*, H. Sakr[1], T. D. Bradley[1†], J. R. Hayes[1], G. T. Jasion[1], E. Numkam Fokoua[1], A. Taranta[1], S.-U. Alam[1‡], D. J. Richardson[1], F. Poletti[1]*

[1]Optoelectronics Research Centre, University of Southampton, Highfield Campus, Southampton, UK.

[†]T. D. Bradley is now with High-Capacity Optical Transmission Laboratory, Eindhoven University of Technology, 5600 MB, Eindhoven, Netherlands.

[‡] S.-U. Alam is now with NKT Photonics Inc., 23 Drydock Avenue, Boston, Massachusetts, MA 02210, USA.

*corresponding authors: L. Xu (l.xu@soton.ac.uk), F. Poletti (frap@orc.soton.ac.uk).

1. Impact of bending losses

We foresee that NANFs will be suitable for practical deployment in a power delivery scenario without significant impact of macro- and micro-bending effects on their low-loss performance as explained in the following.

Based on our simulations, the macro-bend loss for the current 1-km NANF has a value of only 0.1 dB/km at the 16 cm bending radius used in the experiment. Supplementary Fig. 1a shows the simulated macro-bend loss as a function of bend radius R_b, for the bend directions resulting in the highest and lowest loss. The loss scales generally as $1/R_b^2$ but remains below 10 dB/km down to R_b = 4 cm as shown in the Figure. Note that such low bend radii are well below the minimum value that may be expected to occur in a power delivery scenario where the fibre is deployed in a protective cable. For example, the silica PCF designed for power delivery[1] requires a bending radius larger than 50 cm to reduce the bending loss to a level comparable to the NANF at only 16-cm bending radius.

Since the simulations in Supplementary Fig. 1a concern a continuously bent NANF, we also investigated the effect of tight single bends. At very low bend radii, effects such as coupling to higher order core modes or phase matching between the core mode and cladding modes may lead to a sharp increase in the loss[2]. To provide a rough estimate of the critical bend radius where such effects might first occur, we subjected the 1-km NANF to single 180° bends of varying bend radius R_b by holding a small section of the fibre between two parallel, movable plates. The NANF is excited with a white light source, and examples of output spectra at selected R_b values are shown in Supplementary Fig. 1b. At R_b < ~4 cm, an oscillatory pattern in the transmission spectrum appears, moving from short to longer wavelengths as R_b is further reduced. This behaviour is attributed mainly to bend-induced coupling between the fundamental and higher order core modes. When the bend radius decreases to R_b ~ 3 cm, it leads to a markedly increased loss of ~2-3 dB at the 1075 nm laser wavelength. In the spectrum for R_b = 2.5 cm a sharp peak at ~940 nm can be observed, indicative of a cladding mode resonance. Note that the rotation of the NANF relative to the bend plane was not controlled in this test. A separate and more thorough study would be required to accurately characterise these effects, which occur at bend radii well below those expected in a cabled delivery fibre.

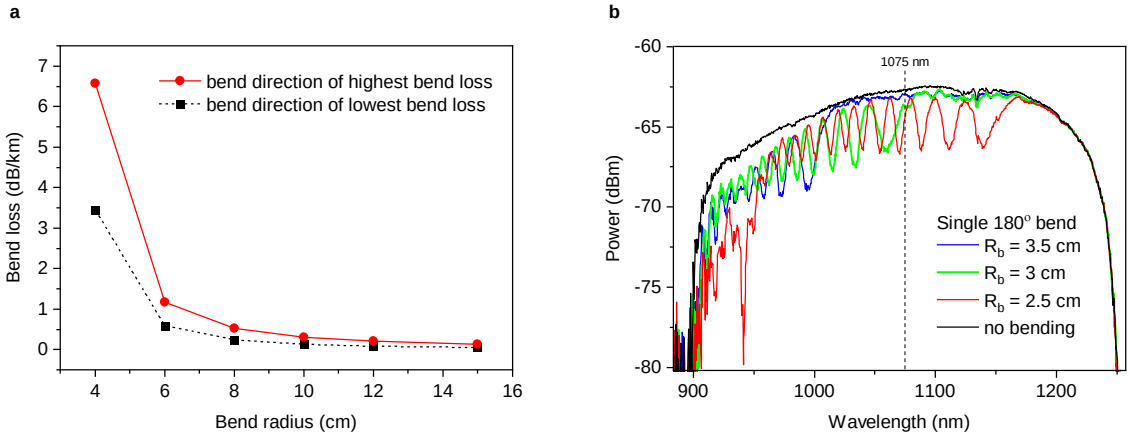

Supplementary Fig. 1 | Bend loss of the 1-km NANF. a Simulated macro-bending loss at 1075 nm vs bend radius R_b, showing the maximum and minimum loss vs the bend direction (angle of bend plane vs the fibre rotation). **b** Effect of a single 180° bend on the transmission spectrum of the 1-km NANF (experimental data). The bend is located ~300m after the NANF input. The bend direction is not controlled.

Concerning micro-bending effects, the NANF was rewound at low tension, thus imposing minimum external stress on the fibre. In practice, the NANF must be cabled which may induce additional stress. In such a situation however, microbending losses due to external perturbations can be minimised by an optimised coating, e.g., by using a dual layer with two materials having low and high Young's moduli[3]. Another method is to increase the stiffness of the fibre by enlarging the glass cladding, as it is done routinely in beam delivery optical fibres for high power operation, where 700 or even 1000 µm fibre diameters are used.

2. Technical improvements needed to realise higher power and longer distance transmission

We envisage that progress in NANF fabrication and improvements of the coupling setup will enable demonstrations of even higher powers and transmission lengths compared to the 1kW-1km result reported here. In terms of NANF propagation loss, the 0.74 dB/km value employed in both the experiment and the simulations is still well above the fundamental loss limits for this fibre type. The NANF fabrication process is being continually refined enabling improved control of the geometrical parameters, leading to further reductions of the propagation loss. Indeed, a 5-tube 2-km long NANF with a record-low 0.3 dB/km loss at 1075 nm was recently reported[4]. As explained in Supplementary Section 3 below, this may further extend the length limits in Fig. 4 (main article) based on a 0.74 dB/km loss value. Note also that a loss value of 0.55 dB/km at 1075 nm in a 6-tube NANF was reported during the course of these experiments, although in a shorter fibre length of about 400 m[5]. Results on kW power delivery in this fibre are included in Supplementary Section 4 in this document.

In terms of improving the laser-to-fibre coupling performance, a first step would be to employ lenses made of high purity grade fused silica with reduced absorption in the near infrared instead of the current "UV grade" fused silica lenses. Paired with an anti-reflection coating with minimal absorption, such lenses should result in a significant reduction in the thermal lensing effects, and hence allow for the high CE of ~95% to be maintained at power levels well above 1 kW. Another

approach is the combination of substrates having refractive index temperature coefficients dn/dT of opposite signs to cancel or suppress the overall thermal lensing of the coupling setup, as employed e.g. in the 10 kW silica-PCF demonstration[6]. An alternative coupling method could be a tapered fibre inserted directly into the hollow core, potentially enabling both low coupling loss and self-stabilisation at high power levels[7,8]. With increasing input powers, thermal management of the coating will also become a necessity due to absorption of the non-coupled light, considering the coating temperature is already exceeding 70 °C at the current input power level of 1.38 kW. Rather than resorting to cooling, it would be preferable to extract the excess light from the cladding before it reaches the coated region of the fibre. Various methods for cladding light extraction (CLE) have been demonstrated, e.g. refs[9,10], and should be applicable to NANF. Another option is to use a low-index coating material to reduce the coupling of light from the cladding, e.g. as in ref[1], although this might in turn require management of residual cladding light at the fibre output.

3. Assessment of limits to further power scaling

This section includes a more detailed description of the numerical simulations used to obtain Fig. 4 in the main article on the scalability of power delivery.

Since the numerical model (see Methods in main article) showed very good agreement with the experimental results, being able to reproduce the small observed red-shift of the spectrum at 1 kW after 1-km NANF propagation with good accuracy (see Fig. 3b,c in the main article), it was used to investigate the scalability to higher power levels and longer NANF lengths. For comparison, simulations were also performed on a state-of-the-art solid core silica fibre designed for near-diffraction-limited power delivery. We selected the silica PCF used for power delivery of 10 kW over 30 m and 1 kW over 300 m[1,6], as these values represent the highest power levels and transmission lengths reported for silica core fibres, to the best of our knowledge. For the NANF, we assumed the same parameters as in our experiment above, including the 0.74 dB/km propagation loss even though lower values can be anticipated (the effect of a recently reported 0.3 dB/km NANF loss

value[4] on the scalability is addressed below). The core is filled with air at atmospheric pressure. For the silica PCF, we used the parameters available from the reports. Instead of the experimentally demonstrated power × distance product of 300 kWm, we used the value 420 kWm which the authors claim is the full potential of the PCF based on the effective mode area of A_{eff} = 2500 μm^2. For simplicity, the core is assumed to support only the fundamental mode, although the actual PCF supports 3 modes. Due to the unavailability of accurate data, the propagation loss and chromatic dispersion were assumed to be dominated by the silica material parameters. This includes a loss value of 0.67 dB/km, corresponding to the Rayleigh scattering limit of silica at the laser wavelength of 1075 nm, and which is slightly lower than the actual value extrapolated from the reported transmissivity (~0.87 dB/km)[1]. We recorded the output spectra of our CW laser source up to its maximum output power of P_{max} = 2.2 kW and used them to model the input signal to the fibre (NANF or PCF). To simulate power levels above this value, the laser spectrum at P_{max} was simply scaled using a constant factor. We simulated power levels up to a value of 5 x P_{max} = 11 kW, comparable to the currently highest commercially available output power of a single-mode CW Ytterbium-doped fibre laser (10 kW). The modelling is described in more detail in Methods in the main article. For simplicity, coupling loss was ignored in these simulations. The evolution of the spectrum over fibre lengths up to 5 km were simulated. Supplementary Fig. 2 compares the evolution of the spectrum vs length for the two fibre types, shown for input powers of P_{in} = 1.4 kW, 2.2 kW, 4 kW, 7.9 kW and 11 kW. Since the fundamental mode propagates in silica in the PCF, and in atmospheric air in the NANF, the spectral evolution is notably different in the two fibres.

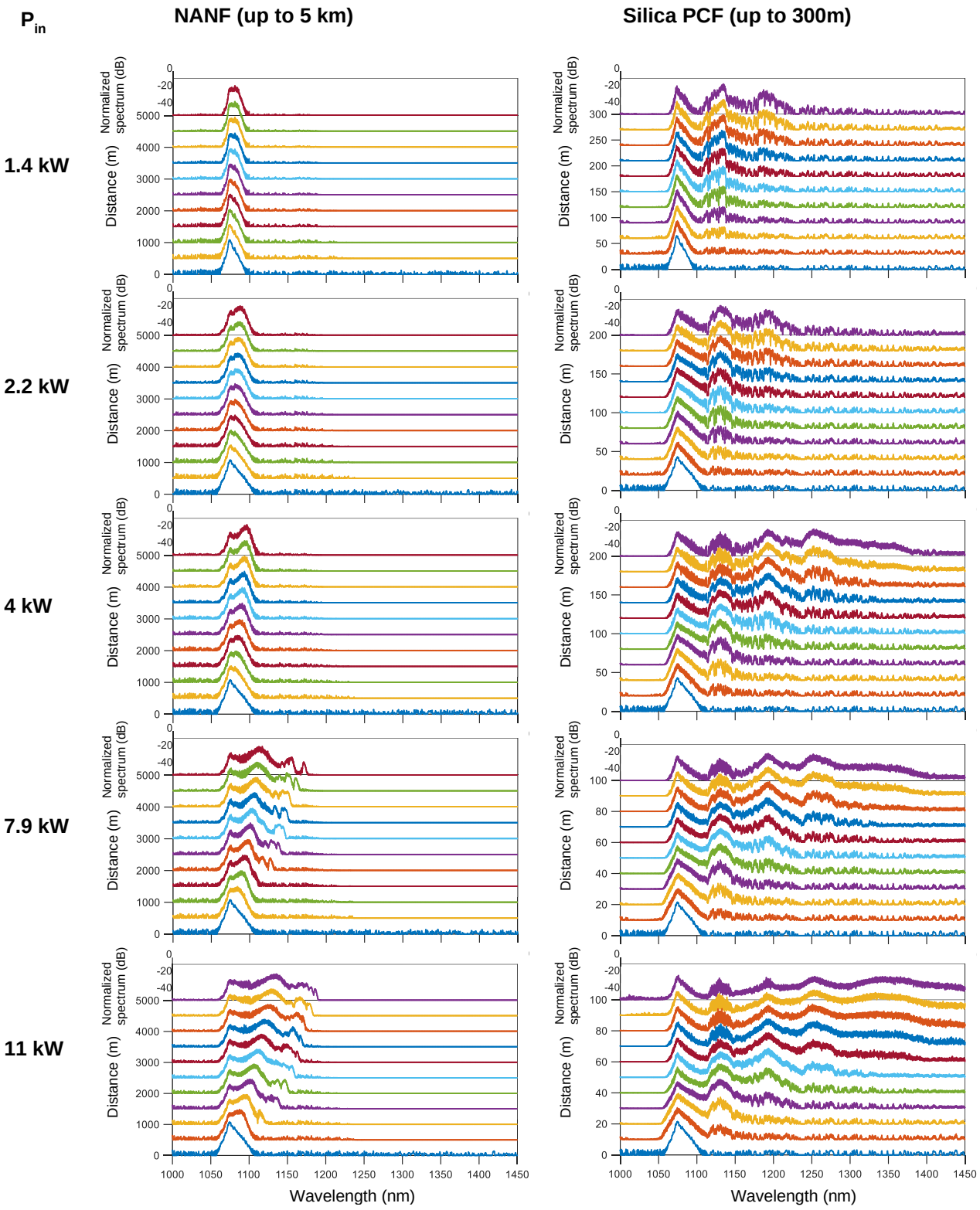

Supplementary Fig. 2 | Simulated spectra vs distance for single-mode CW power delivery in NANF vs silica PCF. For both fibre types, the spectra are calculated for input powers of P_{in} = 1.4, 2.2, 4, 7.9 and 11 kW as indicated in the left column. Note that the range of distances shown differs between the plots, as the spectral broadening vs distance depends strongly on the fibre type and input power.

In the PCF, the vibrational Raman response of silica with a Stokes shift of about 440 cm^{-1} leads to a strong spectral broadening via the formation of several Stokes waves in the first 100 m of propagation. In the air-filled core of the NANF, the Raman response is dominated by rotational transitions of nitrogen having significantly smaller Stokes shifts, leading instead to a gradual broadening of the spectrum to the long-wavelength side (red shift). Consider, for example, the case of P_{in} = 11 kW as shown in the last column of Supplementary Fig. 2. Here, the spectral broadening in the NANF remains substantially lower than in the PCF for similar propagation lengths; a length of 5 km in the NANF produces a spectral broadening comparable to less than 100 m in the PCF. It should be noted that the effect of loss becomes significant after a few km (e.g., the power is reduced by 50% after 4 km in the current NANF with 0.74 dB/km loss).

We observed no signature of the vibrational Raman transitions of oxygen and nitrogen, neither in the experiment nor in the simulations, which is mainly attributed to the fact that the corresponding Stokes wavelengths lie outside the low-loss transmission window, see Fig. 1b in the main article. Note also that, while the NANF has anomalous dispersion at the laser wavelength (see Fig. 1b in the main article), the Raman effect is the main contributing factor to the broadening in comparison to other nonlinear effects raised from the Kerr nonlinearity. For example, the effect of modulational instability (MI) in the air-filled core is found to be negligible relative to the Raman effects. This is confirmed by standard expressions for the bandwidth and peak gain for MI[11]. Using the parameters of our experiment (λ = 1075 nm, P_{in} = 1.4 kW, β_2 = −1.6 ps^2/km, $\gamma = 5.17\times10^{-4}\,W^{-1}km^{-1}$), we find a peak gain of ~1.5 km^{-1} at ±0.58 nm relative to the laser wavelength. Firstly, the MI gain bandwidth is smaller than the laser output spectrum width of ~5 nm. Furthermore, the MI gain is about an order of magnitude smaller relative to the gain of the rotational Raman gain which therefore dominates the spectral broadening through the NANF. This dominance is clear in the simulation results (Supplementary Fig. 2), which are based on a comprehensive model of linear (i.e. dispersion) and nonlinear effects (i.e. Kerr and Raman).

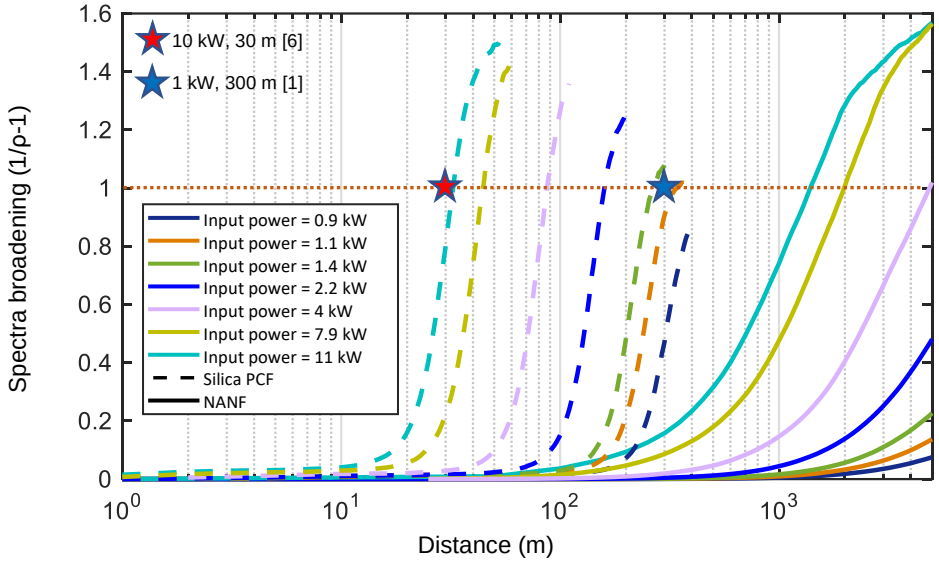

Supplementary Fig. 3 | Simulations of single-mode CW power delivery in silica PCF and NANF: spectral broadening vs distance for various input powers (PCF: dashed lines, NANF: solid lines). The spectral broadening is calculated as a 1/ρ-1, where ρ is a power spectrum overlap ratio – see Methods. The maximum tolerated spectral broadening is set to a value of 1 (ρ=0.5), indicated by the horizontal dotted line. The silica PCF simulations show good correspondence with the demonstrations reported in refs[1,6] as indicated by stars in the figure. Note: the power-distance product for the reported PCF (300 kWm) is slightly lower compared to the full potential of the PCF (420 kWm) which is used in our simulations.

To quantify the spectral broadening and enable comparison between the PCF and the NANF, we adopted a spectral power overlap ratio function ρ, see Methods. In a silica fibre, the critical input power for SRS is defined as the input power leading to equal amounts of power at the pump and Stokes wavelengths. This condition corresponds to $\rho = 0.5$, which we therefore used to define the critical spectral broadening both for the PCF and the NANF. Supplementary Fig. 3 compares the spectral broadening (plotted as $1/\rho - 1$) vs length for the NANF and PCF for various input power values up to 11 kW (including those shown in Supplementary Fig. 2). For each input power level, the maximum permissible propagation length is found where the spectral broadening reaches the critical level (indicated by a horizontal line). Note that the power overlap calculation for the PCF predicts a maximum length of ~30 m at P_{in} = 11 kW and ~300 m at P_{in} = 1 kW, which corresponds well with the reported values as indicated in the figure. Fig. 4 in the main article shows the results for maximum propagation length plotted vs output power for the air-filled NANF (air-NANF), the silica PCF, and a standard SMF, clearly illustrating the significantly extended reach achievable with

the air-NANF. For example, a maximum length of 1180 m is predicted for P_{out} = 10 kW for the air-NANF, a factor 28 improvement relative to the maximum of the PCF which is 42 m (or a factor 40 relative to the experimental PCF demonstration of 10 kW over 30 m). For lower output powers, the improvement factor reduces due to the influence of loss in the NANF. A 1 kW output power can be delivered over a distance of 6870 m, although it should be noted that an input power of 3.3 kW is required. This represents an improvement by a factor 17 relative to the PCF maximum of 407 m, or a factor 23 relative the experimental PCF result of 1 kW over 300 m. It must be noted that since the current simulations assume that the core only supports a single mode, they do not provide any information on potential beam degradation in a real fibre which may support a few, but lossy higher order modes. Although no detrimental effect on beam quality was observed in our demonstration of 1 kW over 1 km, future experiments are needed to confirm that this remains the case at power levels and lengths approaching the limits identified through the simulations where the SRS is higher.

Next, since the limitation in air-filled NANF is set by SRS in air, we also ran simulations where the air is replaced by a vacuum (denoted vacuum-NANF). We observed no spectral broadening up to the highest simulated input power of 11 kW, which is attributed to the negligible overlap of the fundamental mode with the glass surround. Hence, a vacuum-NANF may potentially enable output powers and transmission lengths even beyond the limit of an air-filled NANF as indicated in Fig. 4 (main article), only limited by the available laser power and the fundamentally achievable propagation loss in the NANF. As an alternative to vacuum for avoiding SRS, the NANF core could be filled with a Raman-inactive gas such as Argon. This could be achieved after the fibre draw, as a postprocessing event, or preferably during the draw itself, by using the desired gas as the pressurisation gas to control the draw. This has the additional advantage that the resulting pressure in the fibre would automatically be less than atmospheric, which reduces all nonlinearities. While Raman effects might be avoided in this way, Kerr nonlinearity in the gas-filled core might instead play a role in broadening the spectrum. As discussed above, for example, the effect of MI might be negligible in the case of an air-filled core where the Raman response dominates and the dispersion

of the fibre leads to narrow-bandwidth MI gain. With a different gas however, the dispersion parameters also change which might lead to a noticeable effect of MI. New simulations would be required to predict the spectral evolution in the case of a Raman inactive gas, which could be a subject for future dedicated works.

Finally, we performed simulations to investigate the effect on the scalability for the air-NANF of a newly reported record-low loss value of 0.3 dB/km[4]. For example, we find that a P_{out} = 10 kW can be delivered over a length of 1310 m, whereas a P_{out} = 1 kW can be delivered over 9640 m. The corresponding lengths in the case of 0.74 dB/km loss were 1180 m and 6870 m, respectively. Hence, the advantage of the lower 0.3 dB/km loss is most significant at lower power levels and longer transmission lengths, where it also enables a notably higher transmission efficiency relative to the already low 0.74 dB/km loss of the current NANF.

4. Power delivery of >1 kW over 10-m and 415-m NANFs with 0.55 dB/km loss at 1075 nm

In preparation for the 1-kW power delivery demonstration reported in the main text on a 1-km NANF (denoted here as NANF-1), tests were conducted on shorter fibre samples from a separate NANF (denoted as NANF-2). The NANF-2 was characterised in detail in a previous publication, see ref[5], where it is denoted as “NANF-A”. It has a similar 6-tube structure to NANF-1, with a core diameter of 32 um and a cladding diameter of 206 um. Most notably, NANF-2 has an even lower propagation loss of 0.55 dB/km at 1075 nm, compared to the 0.74 dB/km of NANF-1. The coupling setup used with NANF-2 was identical to Fig. 2 (main article), although a different set of lenses were used. The lens form and substrate was identical to those employed in Fig. 2, but the coating was of a broadband-type (f_1: Thorlabs LA4148-B with 50-mm focal length, f_2: Thorlabs LA4725-B with 75-mm focal length). At the output of the fibre, only the power was measured. The spectra were not measured and the output mode imaging setup in Fig. 2 (main article) had not been implemented. Otherwise, the experimental procedure was as described in Methods. First, a short 10-m sample of

NANF-2 was used for alignment of the coupling system, after which the full available length of 415 m of NANF-2 was tested. The results can be seen in Supplementary Fig. 4, showing the output power (P_{out}) and throughput efficiency (TE = P_{out}/P_{in}) vs input power (P_{in}). Note that the step-like increases in TE observable in the figure occur when the NANF input tip is shifted to compensate for the thermal lensing. For the 10-m NANF-2, a maximum P_{out} = 1296 W was achieved for P_{in} = 1409 W, corresponding to a TE = 92%. At the lower power levels before onset of thermal lensing a TE = 95% is achieved, mainly limited by coupling efficiency (CE) since the propagation loss is negligible over 10 m. The CE drop to 92% at the highest input power is attributed to thermal-lensing related beam distortion that could not be compensated by shifting the NANF input tip. For the 415-m NANF-2, a maximum P_{out} = 1230 W was achieved for a P_{in} = 1358 W, corresponding to a TE = 90% or total loss of 0.46 dB. Here, 0.23 dB is attributed to propagation loss, measured to 0.55 dB/km using the cutback method in a separate experiment[5]. The remaining 0.23 dB is attributed to coupling loss, corresponding to a 95% coupling efficiency. For the 415m NANF-2, no noticeable drop in TE at higher input powers due to thermal lensing effects was observed. The reason for this difference in behaviour between the two fibre samples is unclear. A possibility is that an optimum position of the 10-m NANF-2 input tip was not successfully achieved at high power levels, hence causing insufficient compensation for the thermal-lensing induced shift of the incoming beam waist. The result of 1.23 kW output power with TE = 90% over the 415 m NANF-2 provides an additional demonstration of the advantage of low-loss NANF fibres for power delivery over considerable distances.

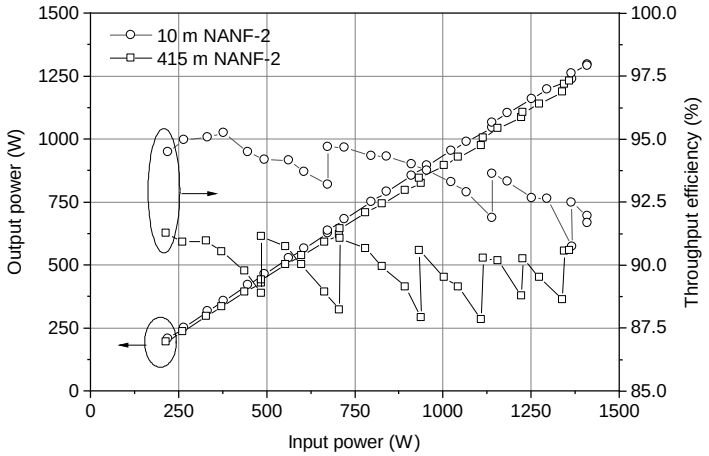

Supplementary Fig. 4 | Power delivery performance for 10-m and 415-m samples of NANF-2 (propagation loss 0.55 dB/km at 1075 nm). Left axis: Output power (P_{out}) vs input power (P_{in}). Right axis: throughput efficiency (P_{out}/P_{in}).

References

1. Matsui, T. et al. Effective Area Enlarged Photonic Crystal Fiber with Quasi-Uniform Air-Hole Structure for High Power Transmission. *IEICE Trans. Commun.* **E103.B**, 415-421 (2020).
2. Setti, V., Vincetti, L. & Argyros, A. Flexible tube lattice fibers for terahertz applications. *Opt. Express* **21**, 3388-3399 (2013).
3. Gloge, D. Optical-fiber packaging and its influence on fiber straightness and loss. *The Bell System Technical Journal* **54**, 245-262 (1975).
4. Sakr, H. et al. Hollow Core NANFs with Five Nested Tubes and Record Low Loss at 850, 1060, 1300 and 1625nm. In *Optical Fiber Communication Conference (OFC) 2021.* Paper F3A.4 (Optical Society of America, 2021).
5. Sakr, H. et al. Hollow core optical fibres with comparable attenuation to silica fibres between 600 and 1100 nm. *Nat. Commun.* **11**, 6030 (2020).
6. Okuda, T., Fujiya, Y., Goya, S. & Inoue, A. Beam Transmission Technology by Photonic Crystal Fiber to Realizes High-precision and High-efficiency Laser Processing Technology. *Mitsubishi Heavy Ind. Tech. Rev.* **57** (2020).
7. Huang, W. et al. Low-loss coupling from single-mode solid-core fibers to anti-resonant hollow-core fibers by fiber tapering technique. *Opt. Express* **27**, 37111-37121 (2019).
8. Xie, S., Pennetta, R. & Russell, P. S. J. Self-alignment of glass fiber nanospike by optomechanical back-action in hollow-core photonic crystal fiber. *Optica* **3**, 277-282 (2016).
9. Yan, P. et al. Kilowatt-level cladding light stripper for high-power fiber laser. *Appl. Opt.* **56**, 1935-1939 (2017).
10. Wysmolek, M. et al. Microstructured fiber cladding light stripper for kilowatt-class laser systems. *Appl. Opt.* **57**, 6640-6644 (2018).
11. Agrawal, G. P. *Nonlinear Fiber Optics*. Third edn (Academic Press, San Diego, CA, 2001).